Fuel 94 (2012) 298–304

Contents lists available at SciVerse ScienceDirect

Fuel

journal homepage: www.elsevier.com/locate/fuel

Steam reforming of methane by rapid compression–expansion

T. Roestenberg [a,b,*], B. Custers [a], M.J. Glushenkov [b], A.E. Kronberg [b], Th.H. vd Meer [a]

[a] University of Twente, CTW/ThW, PO Box 217, 7500 AE Enschede, The Netherlands
[b] Energy Conversion Technologies BV, PO Box 217, 7500 AE Enschede, The Netherlands

ARTICLE INFO

Article history:
Received 11 April 2011
Received in revised form 19 October 2011
Accepted 19 October 2011
Available online 13 November 2011

Keywords:
Chemical reactors
Energy
Process control
Pulsed compression reactor
Reaction engineering
Simulation

ABSTRACT

The concept of using rapid adiabatic compression–expansion for doing chemical reactions promises to be an energy efficient alternative to conventional chemical reactors. In this article, the production of synthesis gas by steam methane reforming using the rapid adiabatic compression–expansion principle is investigated. This was done experimentally as well as with simulations. The experiments were done by means of a single shot reactor, with great control over the reactant composition, reactor temperature and reciprocation path. Simulations were done with an ideally stirred tank reactor model using detailed chemical kinetics. Experiments were done with different mixtures and at various initial temperatures. Simulation results show very good agreement with the experimental data, with the exception of soot formation which was not included in the simulations, and give great insight into the reaction processes that occur within the one cycle.

1. Introduction

Many chemical processes require high temperatures to increase reaction rates and selectivity. In most cases these high temperatures are generated by the combustion of fossil fuels. Recovery of the heat generated requires expensive high temperature recovery equipment and is invariably associated with large energy losses and degradation.

If adiabatic compression is used to generate the heat required for chemical conversion, the energy spent for heating the reactants by compression can simply be recovered from the products by letting the products perform work during expansion. If both compression and expansion are done (nearly) adiabatically, almost no energy losses or energy degradation will occur. The diesel engine is an example of the utilization of the compression principle for heating reactants (although it must be said that the compression and expansion in an internal combustion engine are not adiabatic).

A great area for the application of the adiabatic compressive heating principle in a chemical reactor is the conversion of methane to more valuable products. The first patents for chemical reactors that utilize the adiabatic compression principle to produce syngas have already been developed in the 1920s [1,2]. Primary research into the use of an engine for the reforming of methane to syngas was performed in 1937 [3]. The suitability of an IC engine for the production of synthesis gas via partial oxidation was proven by Karim et al. [4–6]. An overview of other free piston compressor applications can be found in the work from Mikalsen and Roskilly [7].

In order to examine the processes occurring in a free piston reactor used as chemical reactor, a single shot reactor (SSR) was developed. This reactor was designed such that one single compression–expansion stroke of a reciprocating free piston reactor can be reproduced. Partial oxidation experiments have already been conducted successfully using the single shot reactor [8]. More information about the SSR can be found in the work by Roestenberg et al. [9,10].

The goal of the experiments and simulations presented in this article were to use a pulsed compression device for steam methane reforming. If successful, preheating the feed to reaction temperatures as well as the use of a catalyst can be avoided.

2. Experimental setup and procedure

2.1. Setup

The experiments performed in this article were done with the same setup as described by Roestenberg et al. [8], with one modification. For a complete overview of the characteristics the reader is referred to the previous article. The modification made to the setup is the ability to inject steam into the reactor as part of the reaction mixture.

The required amount of demineralized water is injected into the preheated reactor, via a precision syringe. The syringe is mounted

Abbreviations: SSR, single shot reactor; SMR, steam methane reforming; PCR, pulsed compression reactor.

* Corresponding author at: University of Twente, CTW/ThW, PO Box 217, 7500 AE Enschede, The Netherlands. Tel.: +31 534892507; fax: +31 534893663.
E-mail address: t.roestenberg@utwente.nl (T. Roestenberg).

0016-2361/$ - see front matter © 2011 Elsevier Ltd. All rights reserved.
doi:10.1016/j.fuel.2011.10.034

to a small *y*-junction that is connected to the top cover of the reactor and to the capillary tube that supplies the gaseous reactants. This is shown schematically in Fig. 1. The stochiometric amount of liquid water that should be injected depends on the initial temperature of the reactor. The initial temperatures in the experiments were 423 and 543 K, initial pressure was atmospheric.

To increase the peak compression temperature, the methane is premixed with argon. At first, the reactor is flushed with methane/argon mixture and a small portion of the demineralised water is injected, to be sure that all dead volume inside the syringe is filled with water. The reactor is flushed again with gas until all superfluous water is removed. The required amount of water is then injected and a small specified volume of gas is used to entrain the water into the reactor, where it evaporates. Next to the experiments with stochiometric steam/carbon ratio also experiments with an increased steam/carbon ration of 2.5 have been conducted, since industry uses steam/carbon ratios between 2 and 3 to decrease solid carbon depletion and increase synthesis gas yield. The composition of both mixtures used can be found in Table 1.

2.2. Data analysis

In the presentation of the data, the following definitions were used to calculate the yield of H_2 and CO and the CH_4 conversion.

$$\zeta_{CH_4} = \frac{f_{inc} \cdot CH_4}{CH_{4,0}}, \quad Y_{H_2} = \frac{f_{inc} \cdot 2 \cdot H_2}{CH_{4,0}}, \quad Y_{CO} = 1 - \frac{f_{inc} \cdot CO}{CH_{4,0}} \tag{1}$$

f_{inc} represents the ratio between the number of moles on the right and left hand side of the reaction. For the CO_2 and solid carbon yield, similar definitions could be composed. It should be stressed that these definitions could result in theoretical hydrogen yields above 1, since the water that is converted into hydrogen is not accounted for. Nevertheless, the definition stated above is used because it allows comparison with the partial oxidation experiments reported earlier [8].

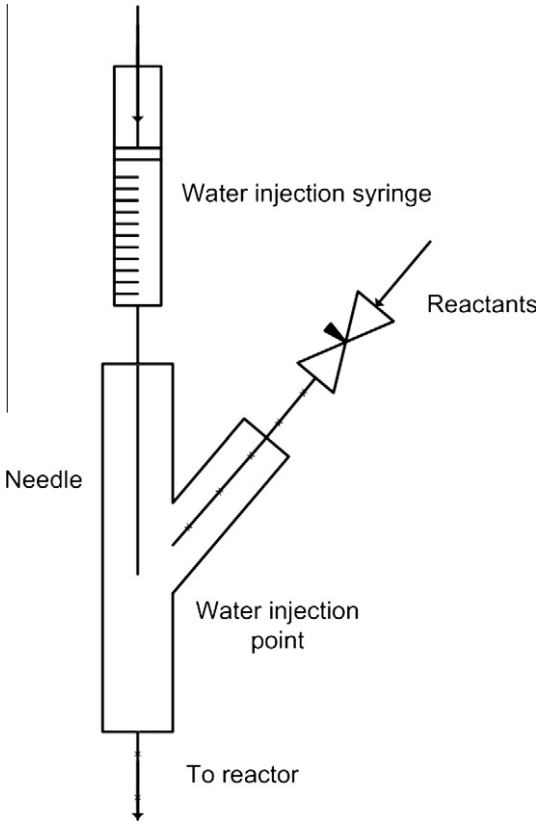

Fig. 1. Schematic overview water injection for steam reforming.

Table 1
Compositions of mixtures used in the experiments.

Mixture	CH_4	H_2O	Ar
1	6.7	6.7	86.6
2	6.1	15.3	78.6

3. Process simulation

The experiments on steam methane reforming have also been simulated using the same simulation method developed for previous publications. The simulation method is described in detail by Roestenberg et al. [8]. The simulation method was employed in this case to simulate the compression and expansion of the mixtures used in the experiments presented in this article. Results of these simulation are included in the results paragraph.

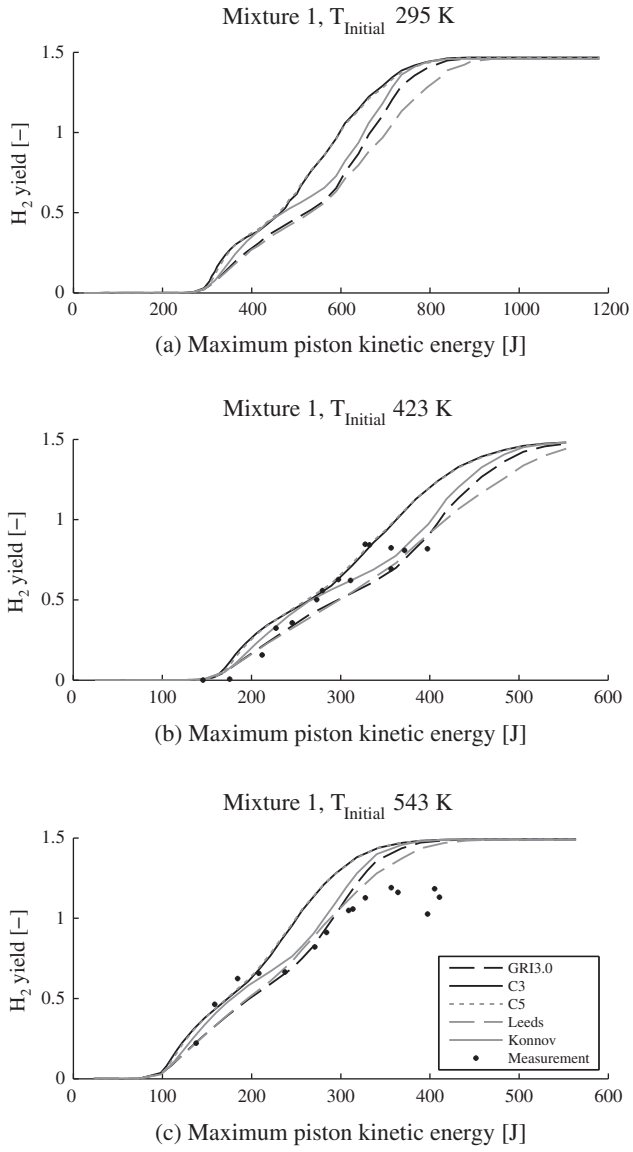

Fig. 2. Hydrogen yield of simulations with mixture 1 and initial temperature 295 K (a), 423 K (b) and 543 K (c) compared to experiments.

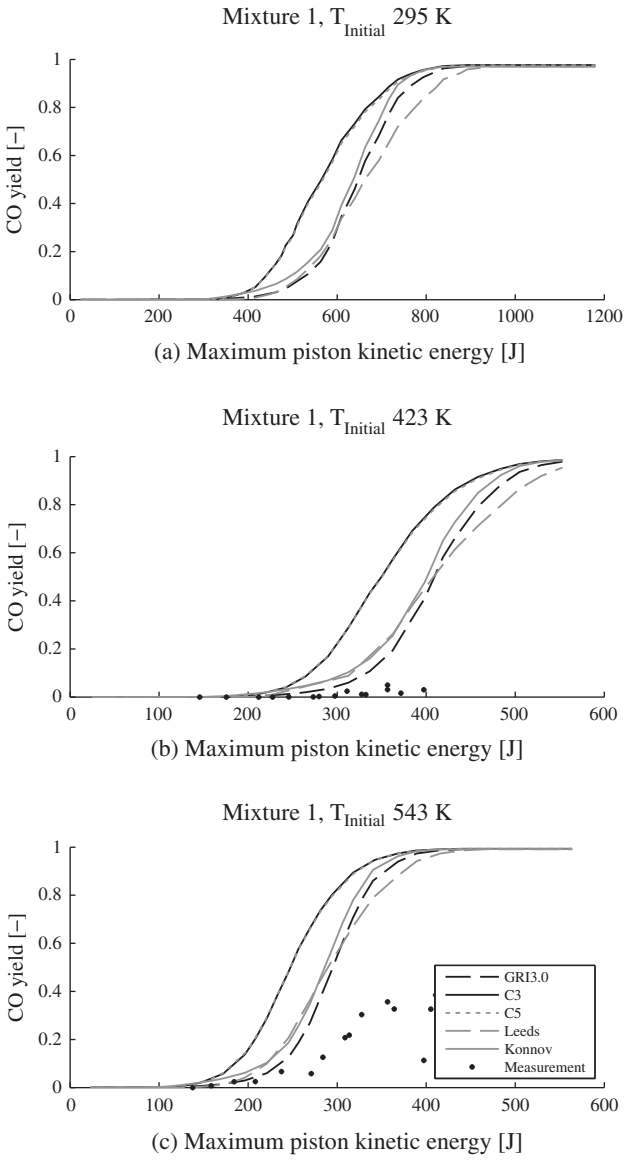

Fig. 3. Carbon monoxide yield of simulations with mixture 1 and initial temperature 295 K (a), 423 K (b) and 543 K (c).

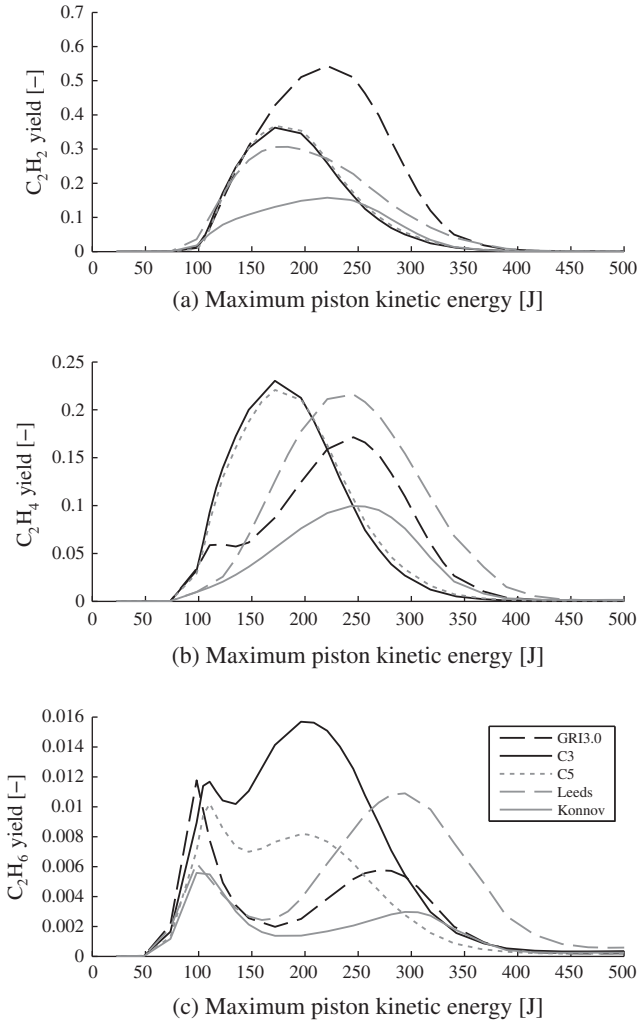

Fig. 4. Acetylene (a), ethylene (b) and ethane (c) yield of simulations with mixture 1 and initial temperature 543 K.

4. Results

Measurements and simulations of H_2 and CO yields as a function of the maximum kinetic energy of the piston have been compared. For both experiments and simulations, the kinetic energy of the piston at the moment when the outlet ports are first opened is a measure for the work exerted on the gas mixture. It was impossible to carry out experiments at ambient temperature, since the steam concentration is higher than the saturated water concentration at room temperature. The 295 K simulations are included nonetheless, to enable comparison with the partial oxidation results.

The experimental results indicated by asterisks in the results graphs represent individual experimental measurements. The quality and repeatability of the measurements can be deduced from the uniformity of the curves that are formed by the individual experimental data points. Repetition of individual results led to a variation in both "output" (such as concentrations of various products and conversion of reactants) as well as "input" parameters (such as piston kinetic energy and peak reactor pressure). However, when output parameters are plotted as a function of input parameters (as is done for all results in this article) this variation reduced to approximately 10% relative.

4.1. Hydrogen yield

In Fig. 2 the conversion of mixture 1 into hydrogen is shown for both simulations and experiments. Whereas the partial oxidation results showed a sudden jump in hydrogen yield after a certain energy threshold [8], the hydrogen concentration rises gradually at energy levels just beyond the energy barrier for the steam reforming case. This is explained by the absence of oxygen in the mixture, so that the fast combustion step observed in the partial oxidation results cannot take place.

The simulations generally agree well with the experimental results, both in energy required to start formation of hydrogen as in the achieved yield (though, similarly to the partial oxidation results, final yields are predicted to be slightly higher). With the stated yield definition, the maximal measured yield to hydrogen is about 120%.

4.2. Carbon monoxide yield

The difference in predicted carbon monoxide yield between measurements and models is much larger than for the hydrogen

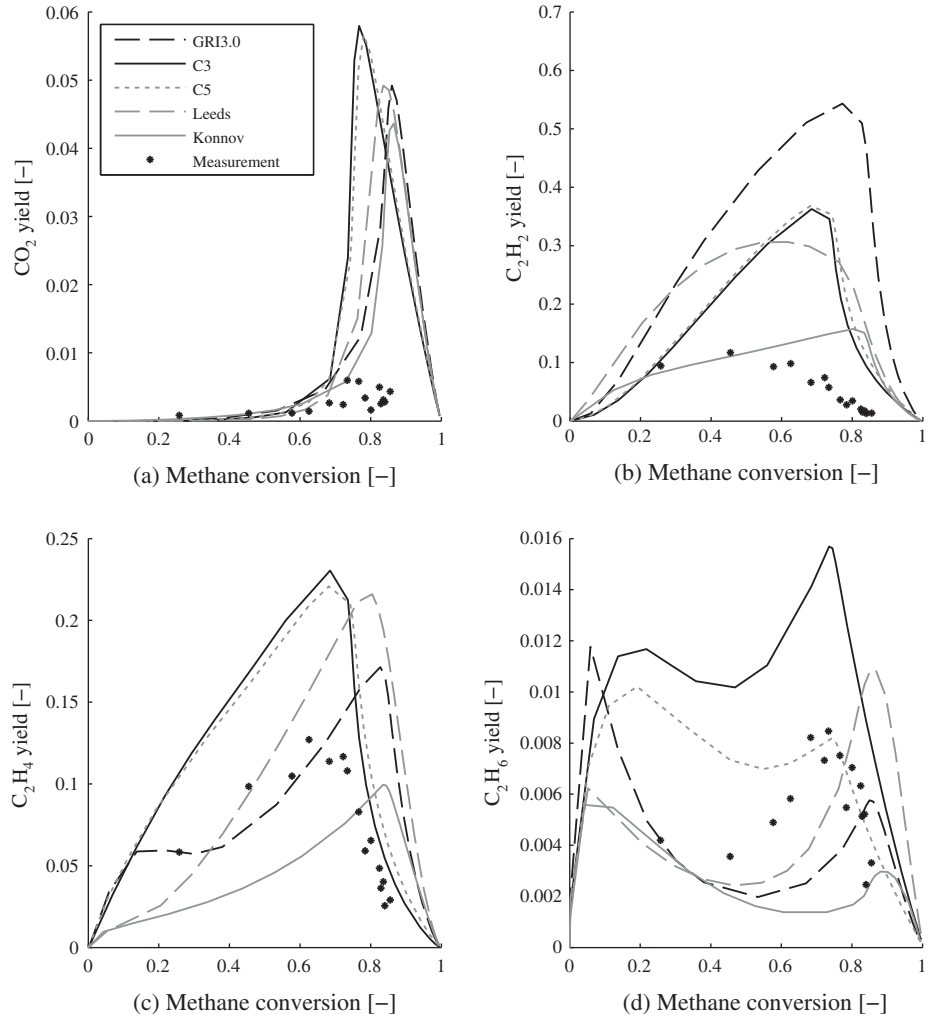

Fig. 5. Secondary species yield by simulations with mixture 1, initial temperature 543 K: CO_2 (a), C_2H_2 (b), C_2H_4 (c) and C_2H_6 (d), compared to experiment.

yield. While the energy threshold for carbon monoxide formation is predicted quite well by some of the models, the CO yields are overestimated by all models. The simulated carbon monoxide yields by steam reforming, together with the experimental results, are shown in Fig. 3.

The difference between measurements and simulations is probably due to the absence of a soot formation model in the different reaction mechanisms used, while quite some carbon depletion was observed in the experiments. A possible route to soot formation is described in the Kassel mechanism [11]:

$$2CH_4 \rightarrow C_2H_6 + H_2 \rightarrow C_2H_4 + 2H_2 \rightarrow C_2H_2 + 3H_2 \rightarrow C(s) + 4H_2 \quad (2)$$

The influence of methane cracking can also be seen in the figures. At 543 K, CO starts to form around 250 J, while H_2 production starts much earlier, already around 100 J. This indicates that at least two separate reaction steps can be identified. The first step, in which no significant amount of CO is produced, can be identified as the methane cracking step that forms hydrogen and a significant portion of soot. The actual reforming step apparently needs more energy and is only initiated after about 250 J for 543 K. From this energy threshold on the actual syngas production starts, represented by the carbon monoxide and additional hydrogen production. At 423 K cylinder temperature there was almost no CO production observed and the hydrogen is thus mainly produced from the thermal decomposition of methane.

The formation of soot reduces the amount of carbon atoms that are available in the gaseous mixture, thus reducing the amount of carbon monoxide formed. The absence of solid carbon formation in the used mechanisms makes much higher carbon monoxide yields possible.

While results in terms of hydrogen yield are quite comparable between models, the differences between the mechanisms are much larger when looking at the carbon monoxide yield. While the C3 and C5 models predict formation of carbon monoxide at piston energy levels just higher than the point where hydrogen is formed, the other three models predict that much more energy is needed for the formation of carbon monoxide. Compared to the experiments, the models, even those that predict more energy needed for steam reforming, predict carbon monoxide to be yielded at lower energy levels than the experiments. However, this difference is small compared to the difference in predicted yield. The experimental yields reach no further than 40%.

4.3. Secondary species

Since ethane, ethylene and acetylene are incorporated in the reaction models, the statement that the thermal decomposition of methane through the Kassel mechanism happens at lower energy levels than the formation of carbon monoxide through steam reforming can be checked using the simulations. In Fig. 4 the ethane, ethylene and acetylene yield results are shown, for the initial

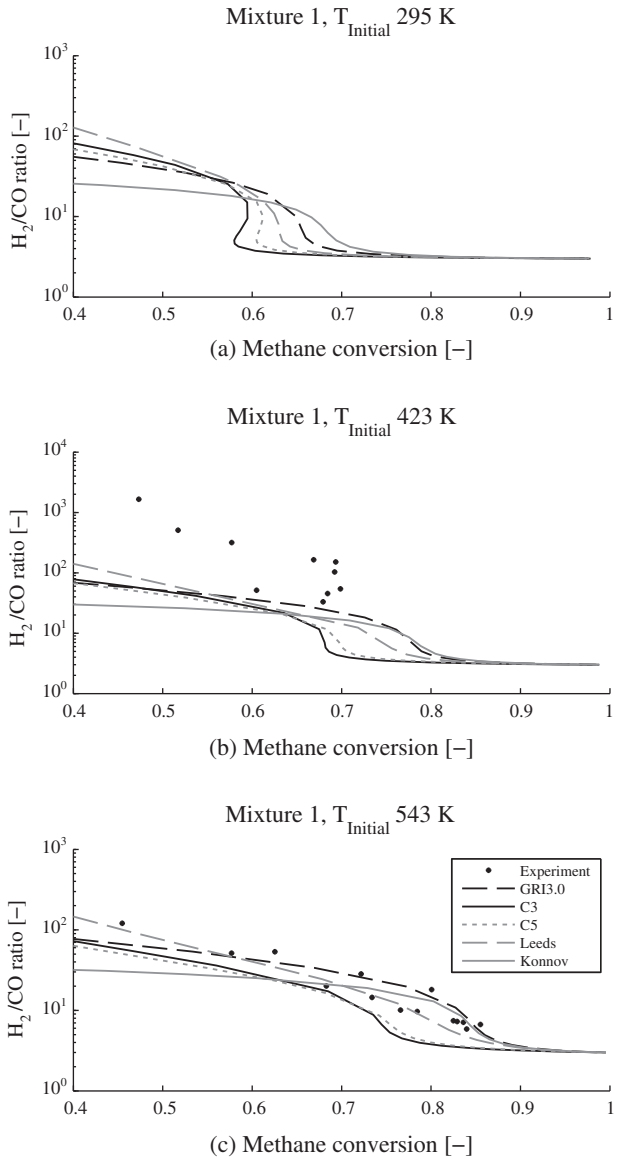

Fig. 6. Hydrogen–carbon monoxide ratio, for mixture 1, initial temperature 293 K (a), 423 K (b) and 543 K (c), compared to simulations.

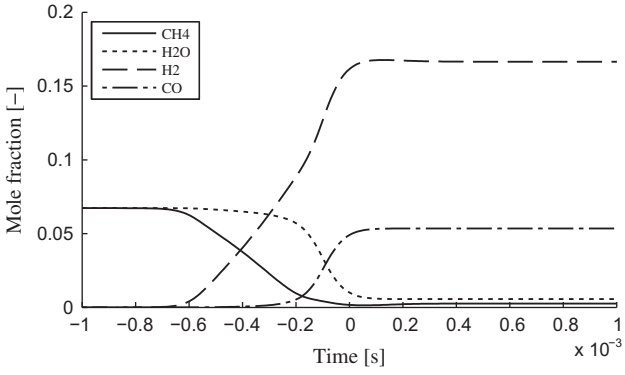

Fig. 7. Major species compression expansion cycle with maximum piston kinetic energy 350 J, simulated by the GRI3.0 mechanism. Initial temperature 543 K.

temperature of 543 K. While the first significant yield of carbon monoxide does not occur before 150–200 J, there is already

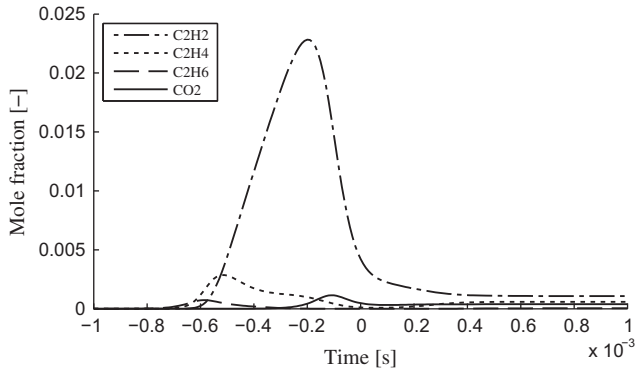

Fig. 8. Secondary species compression expansion cycle with maximum piston kinetic energy 350 J, simulated by the GRI3.0 mechanism. Initial temperature 543 K.

significant ethane yield between 50 and 100 J. This supports the theory that the decomposition of methane through the Kassel mechanism happens before significant steam reforming.

Fig. 5 shows the concentrations of the secondary species, both for measurements and simulations. Results are plotted against the conversion of methane, so that the progress of the reactions is represented on the horizontal axis. It is again evident that ethane is formed right at the beginning of the first conversion of methane. Another interesting result is the lack of carbon dioxide predicted. All models predict that only at one specific conversion a significant quantity of carbon dioxide is formed. And even then, it is much less than the yields that are obtained by partial oxidation.

The experimental results show, just like in the partial oxidation results [8], best correspondence to the Konnov mechanism. Yields of ethylene and acetylene are predicted best by the Konnov mechanism, while the yield of ethane on the other hand is predicted to be lower than the experimental results. In the case of ethane the results correspond best to the Leeds mechanism. Experimental carbon dioxide production is much lower than the predicted highest yield by all mechanisms.

4.4. Hydrogen–carbon monoxide ratio

Since the operating window of the steam reforming process in the PCR contains a part where hydrogen is formed without the formation of carbon monoxide, the hydrogen–carbon monoxide ratio is very high in this region. This is shown in Fig. 6, where the hydrogen carbon monoxide ratio is plotted with a logarithmic *y*-axis and only the part of the results from 40% methane conversion and upwards is shown.

The results of the 543 K initial temperature series show good correspondence with the models, while the 423 K initial temperature series deviates significantly. This is most likely caused by the increased amounts of soot that are formed at lower reaction temperatures, influencing the carbon monoxide yield more severely in the 423 K initial temperature series.

4.5. The steam reforming process

The use of transient simulations to model the chemical reactions inside the single shot reactor not only allows one to study overall yields and conversion, but also provides insight in the evolution of the species over the compression expansion cycle. Fig. 7 shows an example of a single cycle, simulated by the GRI3.0 mechanism. It is again evident that in the first part of the process methane is thermally decomposed, without effecting steam concentration and carbon monoxide formation. The real syngas production, paired

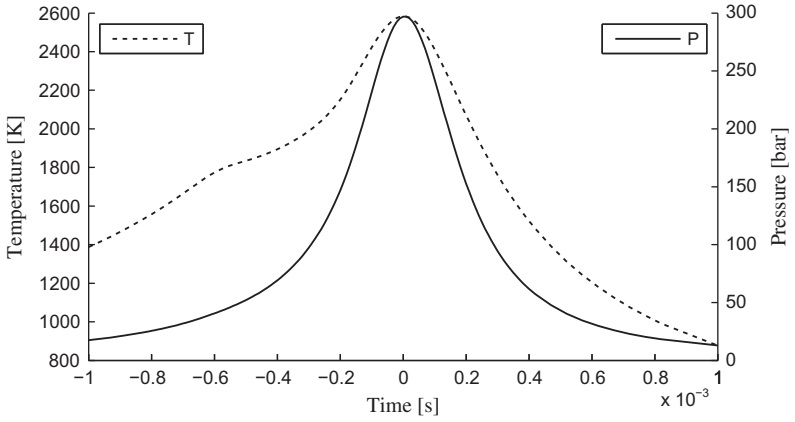

Fig. 9. Temperature and pressure development inside the reactor chamber, simulated by the GRI3.0 mechanism. Initial temperature 543 K.

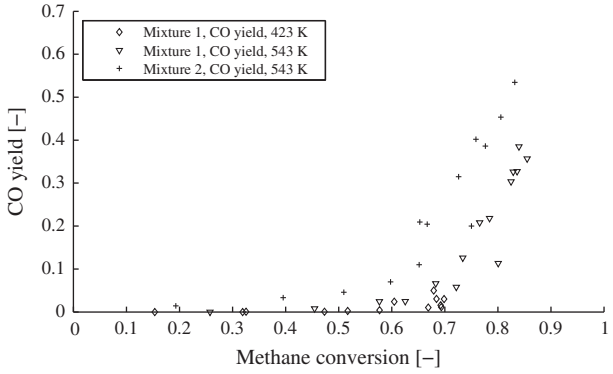

Fig. 10. CO yield of experiments with mixtures 1 and 2 at initial temperature 543 K.

with the disappearance of steam, only starts about 0.4×10^{-3} s before top dead center.

In Fig. 8 the concentrations of the different side products, as simulated by the GRI3.0 mechanism are shown. In this plot the formation in the order, as predicted by the Kassel mechanism can be seen again. The first component to form is ethane, followed by ethylene and finally acetylene. All species are predicted to drop to lower concentrations again as the process continues. The carbon dioxide forms just before top dead center and decreases somewhat near towards the end of the cycle.

To visualize the operating window in which the obtained results are valid, the temperature and pressure histories obtained with the specific 350 J transient simulation are shown in Fig. 9. Temperatures well above 2000 K and pressures of 300 bar can easily be obtained inside the SSR. The transition to the endothermic pure steam reforming reaction is visible in the temperature dip just after 0.6 ms before top dead center ($t = 0$).

Compared to a partial oxidation cycle, the time scale of the processes that happen in the steam reforming cycle is much longer, even though a comparable amount of energy is supplied. While a partial oxidation process at 543 K with 350 J piston kinetic energy is carried out in an order of magnitude of 10^{-4} s [8], the timescale of a similar steam reforming process is expressed in 10^{-3} s.

4.6. Excess steam

To verify if the addition of extra steam can be used to increase synthesis gas yield of the SSR, experiments have also been conducted with 2.5 times the stochiometric S/C ratio (mixture 2). Again, the hydrogen yield is well predicted with the simulations. Carbon monoxide production is over predicted, but differences are a bit smaller than in the stochiometric case. This supports the theory that differences are due to the formation of carbon, because less carbon is depleted when mixture 2 is used. This is shown in Figs. 10 and 11, where CO and C(s) yields are plotted against the conversion of methane for both the stochiometric experiments and the situation with excess steam. The Figures show that extra CO is produced when a certain amount of methane is converted, the result being less soot calculated from the C-atom balance. Excess steam can thus be used to decrease the selectivity towards solid carbon.

5. Discussion

The significant amounts of soot, yielded by the methane cracking reactions may be undesirable for the continuous operation of a pulsed compression device. Solid carbon formation can be reduced by the addition of extra steam, as been demonstrated in the experiments. The addition of oxygen can be used to decrease coke deformation further. Higher reaction temperatures, pressures and quenching rates of the piston are other means to reduce the formation of solid carbon.

Both experiments and simulations suggest that pure cracking of methane (without the addition of steam or oxygen) is also feasible with the current setup. In this case the desired products would be ethane, ethylene, acetylene and hydrogen gas. The tuning of the compression and expansion rates, as well as the cycle length and initial temperature would enable one to reduce the formation of soot, or even avoid soot formation all together.

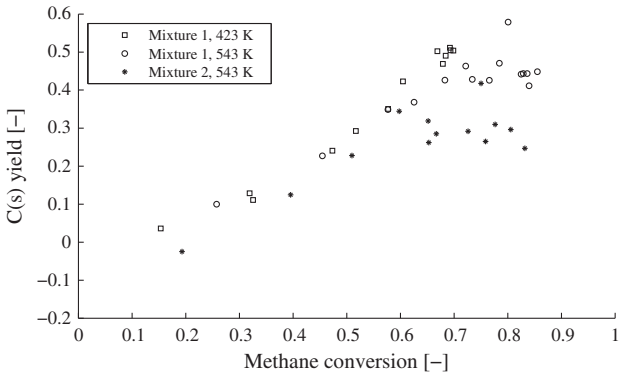

Fig. 11. Solid carbon yield of experiments with mixtures 1 and 2 at initial temperature 543 K.

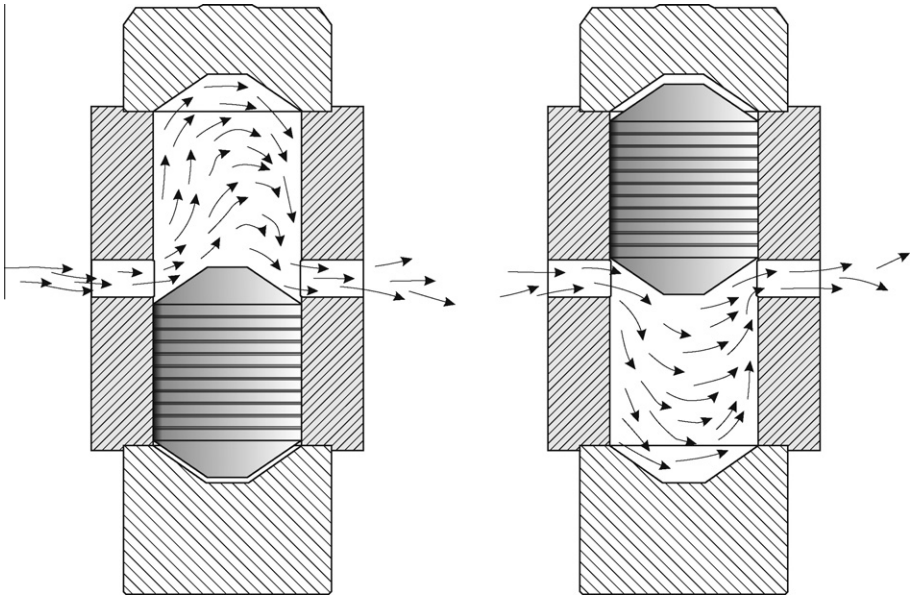

Fig. 12. Pulsed compression reactor principle. Two limiting positions of the reciprocating piston are shown.

A possible application of the chemical process outlined in this article is a continuously operated free piston reactor, such as the version proposed by Glouchenkov in the 1990s [12]. This reactor implements the principle of adiabatic compression in a radically new compression expansion reactor. The PCR is a free piston impulse compression device. It rapidly compresses the reactants by a free piston reciprocating inside a cylinder with a very high frequency (up to 400 Hz). Due to the compression the reactants are heated to very high temperatures and react nearly instantly. A schematic view of the PCR is shown in Fig. 12. Reactants are injected, and products removed, through ports in the side of the reactor, when the piston is in one of its extreme positions.

Experimental results presented in this article show that the application of a PCR for the steam reforming process may be a feasible, much more energy efficient alternative for conventional syngas production processes.

6. Conclusions

Both experiments and simulations have shown that for the temperature and pressure ranges described in this work, pure steam reforming within the single shot reactor is possible. Initial temperature can be very low compared to industrial standards, which means that a great improvement is made in terms of energy efficiency. A clear distinction between the thermal conversion of methane and the steam reforming reactions was observed. Methane decomposition already starts at lower energy levels, while the desired steam reforming reaction is dominating in the higher kinetic energy input range.

The simulation mechanisms used are well capable of predicting the hydrogen yield of the steam reforming process inside the SSR. However, the carbon monoxide concentration is grossly over predicted by all models. The over prediction of the carbon monoxide yield can be attributed to the absence of soot formation mechanism in the used models.

References

[1] Humphrey HA. Apparatus for producing nitric oxide. US Patent 1429035; 1922.
[2] Brutzkus M. Apparatus for chemical production and research. US Patent 1586508; 1926.
[3] Kobozev NI, Derevyanko IG, Stezhinskii AI. The explosive conversion of methane, Part 1. In: Kazarnovskii Ja S, Derevyanko IG, Stezhinskii AI, Kobozev NI. The explosive conversion of methane Part 2. Akad. Nauk S.S.R. Moscow; 1956. p. 133–52.
[4] Karim GA. The production of synthesis gas and power in a compression ignition engine. J Inst Fuel 1963:98–105.
[5] Karim GA. Production of synthesis gas and power in reciprocating internal combustion engines. Br Chem Eng 1963;8(6):392–6.
[6] Karim GA, Moore NPW. The production of hydrogen by the partial oxidation of methane in a dual fuel engine. SAE Technical Paper Ser, No. 901501; 1990.
[7] Mikalsen R, Roskilly AP. A review of free-piston engine history and applications. Appl Therm Eng 2007;27:2339–52.
[8] Roestenberg T, Glushenkov MJ, Kronberg AE, Verbeek AA, vd Meer Th.H. Experimental study and simulation of syngas generation from methane in the Pulsed Compression Reactor. Fuel; 2010. doi: 10.1016/j.fuel.2010.11.002.
[9] Roestenberg T, Glushenkov MJ, Kronberg AE, Krediet HJ, vd Meer ThH. Heat transfer study of the pulsed compression reactor. Chem Eng Sci 2009.
[10] Roestenberg T, Glushenkov MJ, Kronberg AE, vd Meer ThH. On the controllability and run-away possibility of a totally free piston, pulsed compression reactor. Chem Eng Sci. doi: 10.1016/j.ces.2010.05.034.
[11] Fridman A. Plasma chemistry. Cambridge University Press; 2008. p. 589–91.
[12] Gluouchenkov M. RU, 2097121, 1997; RU, 2115467, 1997; RU, 2142844, 1999.